



1 **Development of an offline Aerosol Mass Spectrometry method for organic aerosol**
2 **characterization in a globally distributed Surface Particulate Matter Network**

3 Yuxuan Ren¹, Randall V. Martin^{1*}, Jhao-Hong Chen^{1#}, Christopher R. Oxford¹, Brent
4 J. Williams^{1,&}, Rodney J. Weber², Lu Xu^{1*}

5 ¹Department of Energy, Environmental & Chemical Engineering, Washington
6 University in St. Louis, St. Louis, Missouri 63130, United States

7 ²School of Earth and Atmospheric Sciences, Georgia Institute of Technology, Atlanta,
8 Georgia 30332, United States

9 [#]now at Bureau of Air, Kansas Department of Health and Environment, Topeka, Kansas
10 66612, United States

11 [&]now at Department of Soil, Water, and Climate, University of Minnesota, St. Paul,
12 Minnesota 55108, United States

13 *Correspondence to: Lu Xu (xu1@wustl.edu) and Randall V. Martin
14 (rvmartin@wustl.edu)

15 **Abstract**

16 Global measurements of organic aerosol (OA) concentrations and chemical
17 composition remain limited and unevenly distributed. While monitoring networks,
18 including the globally distributed Surface Particulate Matter Network (SPARTAN),
19 provide an established framework for measurements, their current methodologies do
20 not fully support comprehensive OA characterization. Aerosol Mass Spectrometry
21 (AMS) is widely used for real-time OA composition measurements, but its cost,
22 complexity, and logistical requirements limit long-term, multi-site online deployment,
23 particularly at the global scale. Here we develop and evaluate an offline AMS
24 methodology to characterize OA in particulate matter collected on Teflon filters
25 routinely used by monitoring networks. Using a commercial ultrasonic nebulizer
26 coupled with a syringe pump, this offline method is highly reproducible, requires small



27 extract volumes (2 mL), offers low detection limits (1.7 μg OA and 0.43 μg sulfate per
28 filter), and achieves higher nebulization efficiency than previous methods. We evaluate
29 this offline AMS method by co-located online AMS observations. We find that
30 oxygenated OA is effectively recovered ($64 \pm 28 \%$) while the recovery is lower for
31 hydrocarbon-like OA due to its limited water solubility. This approach offers new
32 capability for SPARTAN and is readily adaptable to other monitoring networks. Its
33 application across networks will broaden the spatiotemporal coverage of AMS-based
34 OA measurements and improve methodological and instrumental consistency to
35 support ongoing efforts to build a long-term, globally consistent OA dataset.

36 1. Introduction

37 Organic aerosol (OA) constitutes a substantial fraction of atmospheric fine particulate
38 matter ($\text{PM}_{2.5}$), contributing approximately 20–90 % of its total mass (Kanakidou et al.,
39 2005; Zhang et al., 2007). OA influences climate through direct aerosol-radiation
40 interactions (Chung et al., 2012) and cloud formation (Sareen et al., 2013), and affects
41 human health due to its high potential to inflict oxidative stress and inflammation by
42 generating reactive oxygenated and nitrogen species (Bates et al., 2019; Tuet et al.,
43 2016). OA originates from both primary and secondary processes. Primary OA (POA)
44 is directly emitted from fossil fuel combustion, biomass burning, and other
45 anthropogenic or natural activities. Secondary OA (SOA) is formed through gas-phase
46 oxidation of anthropogenic and biogenic volatile organic compounds (VOCs) and
47 subsequent condensation or nucleation (Jimenez et al., 2009; Kroll and Seinfeld, 2008).
48 The large number of molecular species and reaction pathways involved leads to extreme
49 chemical complexity, complicating the characterization of OA loadings, spatiotemporal
50 variability, and atmospheric oxidation processes (Kroll et al., 2011; Williams et al.,
51 2007).

52 Despite advances in instruments capable of detailed chemical speciation, global OA
53 concentrations and chemical composition remain poorly constrained (Sun et al., 2025).
54 Measurements are largely derived from independent field campaigns that vary in



55 instrumentation, sampling objectives, and methodologies, and are typically confined to
56 limited time periods. In addition, these measurements are mostly conducted in
57 developed regions in the northern midlatitudes, with relatively sparse representation
58 from the Global South (Jeon et al., 2023; Tsimpidi et al., 2025). Therefore, global OA
59 datasets compiled from collections of unique field campaigns face challenges such as
60 limited comparability and incomplete spatiotemporal coverage, which further inhibit
61 accurate evaluation of global OA simulations in chemical transport and climate models
62 (Pai et al., 2020; Shrivastava et al., 2017). This highlights the need to routinely and
63 consistently measure OA concentrations and composition across long-term monitoring
64 networks of sites, particularly at the global scale.

65 The Surface Particulate Matter Network (SPARTAN, [https://www.spartan-](https://www.spartan-network.org/)
66 [network.org/](https://www.spartan-network.org/)) collects PM_{2.5} on Teflon filters from globally distributed sites that
67 prioritize undersampled, densely populated regions. This network provides long-term,
68 ground-based PM_{2.5} composition measurements, including black carbon (BC), trace
69 elements, water-soluble ions, and organic carbon (OC), to support the development and
70 evaluation of satellite-based PM_{2.5} estimates (Liu et al., 2024; McNeill et al., 2020; Ren
71 et al., 2025; Snider et al., 2015, 2016; Weagle et al., 2018). Its consistency across
72 globally distributed sites offers the possibility of constructing a comprehensive global
73 OA dataset. Leveraging this potential, however, requires targeted methodological
74 development to enable comprehensive OA characterization within the network.

75 The Aerodyne High-Resolution Time-of-Flight AMS (HR-ToF-AMS) has been
76 extensively used for real-time measurement of OA with high time resolution and
77 sensitivity in field campaigns (DeCarlo et al., 2006). By coupling thermal vaporization
78 with 70 eV electron ionization (EI), AMS provides quantitative mass spectra of non-
79 refractory aerosol components, including OA, sulfate, nitrate, ammonium, and chloride
80 (Canagaratna et al., 2007). However, its high cost, operational complexity, and
81 logistical requirements limit its feasibility for long-term, simultaneous deployment
82 across multiple sites. This has stimulated the development of offline AMS methodology,



83 where atmospheric samples are collected in the field and subsequently atomized for
84 AMS analysis in the laboratory. Previous studies have demonstrated the promise of
85 offline AMS for quantitative OA characterization. Sun et al. (2011) analyzed water
86 extracts of PM_{2.5} in the southeastern US to determine water-soluble organic matter to
87 organic carbon (OM/OC) ratios using AMS, complemented by total organic carbon
88 (TOC) measurements of water-soluble OC. Mihara and Mochida (2011) investigated
89 extraction with multiple solvents (water, methanol, and ethyl acetate) for PM collected
90 in urban Nagoya, Japan, using phthalic acid as an internal standard (IS) for
91 quantification. Daellenbach et al. (2016) systematically assessed water-extract offline
92 AMS and quantified source-related OA recoveries through comparison with co-located
93 online measurements in Paris and Zurich. To extend applicability to lower mass
94 loadings, O'Brien et al. (2019) introduced a small-volume nebulizer for microgram-
95 level analysis with IS-based calibration slopes, while Niedek et al. (2023) developed
96 another micronebulization technique with improved detection limits for PM collected
97 from uncrewed platforms. To further improve OA recoveries, Vasilakopoulou et al.
98 (2023) proposed excluding filtration during water extraction to retain partially soluble
99 and insoluble OA fractions, and Khare et al. (2025) demonstrated improved OC
100 recovery using organic solvents, with high similarity between online and offline mass
101 spectra. Beyond methodological development and evaluation, offline AMS has been
102 directly applied to characterize long-term OA concentrations and infer source
103 properties across sites in Europe (Bozzetti et al., 2016, 2017a, 2017b; Casotto et al.,
104 2022, 2023; Daellenbach et al., 2017; Moschos et al., 2022; Srivastava et al., 2021;
105 Vlachou et al., 2018, 2019), US (Niedek et al., 2025), China (Cui et al., 2024; Ge et al.,
106 2017; Huang et al., 2014; Li et al., 2021; Qiu et al., 2019; Xu et al., 2015; Ye et al.,
107 2017a, 2017b), and India (Bhowmik et al., 2024; Cash et al., 2023).

108 Despite these developments, offline AMS has not been integrated as a routine
109 measurement within globally distributed monitoring networks. For application within
110 large-scale networks, the offline method is expected to meet several criteria: it should



111 efficiently generate particles from small volume extracts given limited filter mass
112 loadings, the setup should be reproducible and easy to maintain for rapid analysis, and
113 the procedures should be compatible with existing protocols within monitoring
114 frameworks. However, existing approaches do not fully satisfy these requirements. For
115 example, the use of customized nebulizers can limit reproducibility, and some
116 configurations require relatively large extract volumes (typically 5–15 mL) or
117 additional operational steps and time to ensure cleaning and stability. In addition,
118 quantification based on internal standard requires rigorous calibration, and the use of
119 externally spiked internal standard (e.g., isotopically labeled ammonium nitrate or
120 ammonium sulfate) may introduce potential interference while increasing sample
121 preparation complexity. Therefore, further development and evaluation are needed to
122 establish a reproducible and operationally streamlined offline AMS method suitable for
123 routine deployment within globally distributed monitoring networks.

124 In this study, we develop an offline AMS methodology well-suited for additionally
125 characterizing water-soluble OA in SPARTAN Teflon filters while sustaining existing
126 measurements, with broader applicability to other monitoring networks that use similar
127 filter-based sampling. We use a commercial ultrasonic nebulizer for high
128 reproducibility and use sulfate as an internal standard given its routine measurement in
129 monitoring networks. We further evaluate this offline AMS method against co-located
130 online AMS measurements. This development of offline AMS methodology establishes
131 a basis for a comprehensive OA dataset with consistent instrumentation and
132 methodology across globally distributed sites in densely populated regions.

133 **2. Methods**

134 **2.1 Chemicals**

135 Ammonium sulfate (AS, American Chemical Society (ACS) grade) and nitric acid
136 (ACS grade) are from Fisher Scientific. Methanol (high-performance liquid
137 chromatography (HPLC) grade), glucose ($\geq 99.5\%$, gas chromatography (GC) grade),



138 DL-4-Hydroxy-3-methoxymandelic acid (HMMA, ≥ 98 % HPLC grade), and
139 poly(ethylene glycol) (PEG-400) are from MilliporeSigma. All solutions are prepared
140 using ultrapure water (Milli-Q water, $18.2 \text{ M}\Omega \cdot \text{cm}$). Prior to use, all glassware is soaked
141 in 1 % nitric acid for 24 hours, rinsed sequentially with methanol and a triple ultrapure
142 water wash, and baked at $500 \text{ }^\circ\text{C}$ for 5 hours.

143 2.2 SPARTAN sampling and chemical analyses

144 SPARTAN is a long-term global network that measures ground-based PM composition
145 at sites distributed across densely populated regions. Detailed descriptions of
146 SPARTAN and its measurements have been described in the literature (Liu et al., 2024;
147 McNeill et al., 2020; Ren et al., 2025; Snider et al., 2015, 2016; Weagle et al., 2018).
148 PM samples are collected on 25 mm Teflon filters (PT25DMCAN-PF03A,
149 Measurement Technology Laboratories, Bloomington, Minnesota, US) assembled in
150 cartridges for use in sampling stations (SS5, AirPhoton, Baltimore, Maryland, US)
151 coupled with a sharp-cut cyclone (SCC1.829, Mesa Laboratories, Lakewood, Colorado,
152 US) typically operated at a target flow rate of 5 L/min for a $\text{PM}_{2.5}$ size cut. Each
153 cartridge consists of seven sample filters and one field blank. Sampling duration is site-
154 specific, ranging from 12 to 48 hours per filter to deposit approximately 100–200 μg of
155 collected aerosol mass.

156 This network routinely provides measurements of PM mass and chemical composition.
157 Filters are equilibrated and weighed before and after sampling under controlled
158 conditions of $21.5 \text{ }^\circ\text{C}$ and 35 % relative humidity. Chemical analysis begins with non-
159 destructive optical techniques, including Hybrid Integrating Plate/Sphere (HIPS) for
160 BC (White et al., 2016), Fourier Transfer Infra-Red spectroscopy (FT-IR) for OC
161 (Debus et al., 2022; Dillner and Takahama, 2015), and X-Ray Fluorescence (XRF) for
162 elements (Liu et al., 2024). Elements, including sulfur, are quantified using an energy
163 dispersive XRF (Epsilon 4, Malvern PANalytical, Worcestershire, UK). Calibration is
164 performed annually, with monthly checks to confirm instrument stability (Liu et al.,
165 2024). Following these non-destructive analyses, filters undergo a destructive



166 extraction in which collected particles are dissolved into solution. Filters are placed
167 aerosol-side up in a 20 mL scintillation vial and covered with 0.2 mL of HPLC-grade
168 methanol followed by 5.8 mL of ultrapure water. The vial is sealed with aluminum foil
169 and a plastic cap and sonicated for 30 minutes at room temperature. Sonication destroys
170 the filter matrix, allowing the collected aerosol to dissolve or become suspended in the
171 extract. The extract is then filtered through a 0.2 μm polypropylene syringe filter. A 4
172 mL aliquot of the filtered extract is refrigerated for Ion Chromatography (IC) analysis
173 to quantify water-soluble ions. Cations including ammonium, and anions including
174 sulfate, nitrate, and chloride, are measured using two IC systems (Dionex Integriion,
175 Thermo Scientific, Waltham, Massachusetts, US). The cation system uses a methane
176 sulfonic acid eluent generation system with a Dionex CS12A column and a CG12A
177 guard column, while the anion system uses a potassium hydroxide eluent generation
178 system with a Dionex AS18 column and AG18 guard column. Calibrations for both
179 systems are performed at the beginning of each measurement sequence using standards
180 prepared biweekly.

181 The remaining 2 mL aliquot of the filtered extract is transferred to a glass vial and
182 immediately frozen for subsequent AMS analysis to characterize OA, which is the focus
183 of this study.

184 **2.3 Offline AMS methodology**

185 Our offline AMS methodology consists of a syringe pump (780100I, Thermo Fisher
186 Scientific Inc., Waltham, Massachusetts, US), a commercial ultrasonic nebulizer (U-
187 5000AT+, Cetac Technologies Inc., Omaha, Nebraska, US), a diffusion dryer, a
188 Scanning Mobility Particle Sizer (SMPS, Model 3938, TSI Inc., Shoreview, Minnesota,
189 US), and an HR-ToF-AMS (Aerodyne Research Inc., Billerica, Massachusetts, US). A
190 simplified schematic of the experimental setup is shown in [Figure S1](#).

191 Filter extracts are delivered by the syringe pump to the ultrasonic nebulizer, where
192 aerosol is generated through oscillation of a piezoelectric transducer operating at 1.4



193 MHz (Ohata et al., 2011). Dry, zero air is introduced near the transducer to generate
194 airflow. The downstream tube heater is turned off to minimize potential volatilization
195 loss of organics, and water vapor is subsequently condensed in a tube maintained at
196 3 °C. The generated particles are then dried using a silica gel diffusion dryer and
197 analyzed by the HR-ToF-AMS and SMPS for chemical composition and size
198 distribution measurements. Figure S2 illustrates the measurement sequence for a
199 SPARTAN cartridge using representative raw AMS data. Field blank filters are
200 analyzed using the same procedure as the sample filters. Each cartridge measurement
201 also includes a laboratory blank with no filter present, with signals used for blank
202 subtraction within the corresponding cartridge. In addition, a 10 mg/L AS solution is
203 analyzed at the beginning and end of each experimental day to verify instrument
204 stability.

205 The choice of the nebulization system is critical for offline AMS methods. Commonly
206 used commercial nebulizers, such as the TSI nebulizer (Model 3076, TSI Inc.,
207 Shoreview, Minnesota, US) (Li et al., 2021; Sun et al., 2011) and the Apex Q nebulizer
208 (Elemental Scientific Inc., Omaha, Nebraska, US) (Khare et al., 2025; Vlachou et al.,
209 2018), typically require relatively large extract volumes, which can be challenging for
210 filters with limited collected mass. Custom nebulization systems (Cash et al., 2023;
211 Niedek et al., 2023; O'Brien et al., 2019) have expanded the capabilities of offline AMS
212 through specialized designs, however, these configurations are not commercially
213 available and may be less accessible for routine implementation. The ultrasonic
214 nebulizer used in this study has been applied in previous studies (Chen et al., 2019;
215 Fang et al., 2015; Xu et al., 2017) and can efficiently nebulize small extract volumes
216 while generating relatively large particles aligned with the AMS transmission
217 efficiency. The system is stable and easy to clean and maintain, with carryover removed
218 by nebulizing ultrapure water between samples within a few minutes (Figure S2), which
219 supports routine analysis of large numbers of samples within monitoring networks.



220 The HR-ToF-AMS operating principles, calibration procedures, and analysis protocols
221 have been described extensively elsewhere (Canagaratna et al., 2007; DeCarlo et al.,
222 2006). AMS provides quantitative mass spectra of non-refractory submicron PM (PM₁)
223 components, including OA, sulfate, nitrate, ammonium, and chloride. In this study, the
224 HR-ToF-AMS is operated in V mode (DeCarlo et al., 2006), providing a mass
225 resolution of approximately 2000–3000 m/Δm and a temporal resolution of 1 minute.
226 AMS data are processed using the standard AMS data analysis toolkits Squirrel v1.67A
227 (SeQUential Igor data RetRIeval) and Pika v1.27A (Peak Integration by Key Analysis)
228 in the IGOR Pro software package (Wavemetrics Inc., Portland, Oregon, US). Values
229 for the AMS nitrate ionization efficiency (IE) and relative ionization efficiencies (RIEs)
230 for sulfate and ammonium are determined through calibration following standard
231 procedures. A default RIE value of 1.4 is assumed for OA (Xu et al., 2018). The
232 chemical-dependent collection efficiency (CDCE) is applied following Middlebrook et
233 al. (2011).

234 We perform positive matrix factorization (PMF) analysis for OA factor apportionment.
235 The principles of PMF have been described in detail elsewhere (Paatero and Tapper,
236 1994; Ulbrich et al., 2009a). Briefly, PMF is a bilinear unmixing receptor model that
237 quantitatively resolves organic mass spectra into a linear combination of static factor
238 profiles and their time-dependent contributions, with each factor attributed to
239 characteristic sources and atmospheric processes. PMF is conducted using the PMF
240 Evaluation Toolkit (PET) v3.08E. Variables with low signal-to-noise (SNR < 0.2) are
241 removed, while “weak” variables (0.2 < SNR < 2) are downweighted by a factor of two
242 (Paatero and Hopke, 2009). Ions including O⁺, HO⁺, H₂O⁺, and CO⁺, which are scaled
243 to CO₂⁺, are also downweighted to prevent excessive weighting of CO₂⁺ (Ulbrich et al.,
244 2009a).

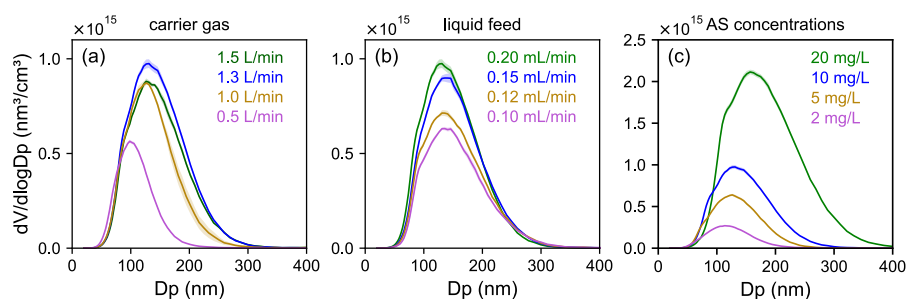
245 3. Results and Discussion

246 3.1 Optimization and characterization of nebulization system



247 We optimize key parameters of the nebulization system, including carrier gas flow rate
248 and liquid feed rate, to generate particles with high transmission efficiency in the AMS
249 and higher mass concentrations (Figure 1). Increasing the carrier gas flow rate enhances
250 aerosol transport and reduces upstream losses, leading to higher particle mass
251 concentrations. However, at sufficiently higher flow rates, dilution by the carrier gas
252 becomes dominant and reduces particle mass concentrations. Varying the carrier gas
253 flow rate (0.5, 1.0, 1.3, and 1.5 L/min) shows a clear increase followed by a decrease
254 in particle mass concentration, with 1.3 L/min identified as optimal. For the liquid feed
255 rate, higher feed rates increase particle mass concentrations due to increased solute
256 delivery. However, increasing the feed rate also reduces the number of AMS runs per
257 sample of a finite extract volume. We vary the liquid feed rate at 0.10, 0.12, 0.15, and
258 0.20 mL/min, and select 0.20 mL/min to maximize particle mass concentration while
259 maintaining an adequate AMS sampling period, providing approximately 10 minutes
260 of measurement time from a 2 mL extract.

261 Under these optimized conditions, we characterize particle size distributions generated
262 from AS solutions at concentrations of 2, 5, 10, and 20 mg/L. These concentrations are
263 selected to represent the range of inorganic ion loadings observed in SPARTAN
264 samples, with 2 mg/L and 20 mg/L corresponding approximately to the 5th and 95th
265 percentiles. Across this range, the regenerated aerosol exhibits a mode electrical
266 mobility diameter (D_m) of approximately 120 to 180 nm (Figure 1c), which aligns well
267 with the AMS transmission efficiency that is nearly 100 % for particles with vacuum
268 aerodynamic diameters (D_{va}) between 70 and 500 nm (Jimenez et al., 2003; Liu et al.,
269 2007).



270

271 Figure 1. Particle size distributions generated from ammonium sulfate (AS)
 272 solutions and measured with a Scanning Mobility Particle Sizer (SMPS) to
 273 optimize nebulization system parameters. Panels show the effects of (a) carrier gas
 274 flow rate, (b) liquid feed rate, and (c) solution concentrations. Colored lines
 275 represent the mean of three runs, with colored shading areas indicating the standard
 276 error. The diameter (D_p) here is the electrical mobility diameter (D_m).

277 3.2 Quantification using internal standard

278 Nebulization efficiency (NE), defined as the ratio of mass measured by the AMS to the
 279 mass of solute nebulized, is a key indicator of offline AMS sensitivity (O'Brien et al.,
 280 2019). To quantify NE, 2 mL of binary solutions containing varying proportions of
 281 sulfate and organic species are nebulized at a fixed total solute concentration of 40 mg/L.
 282 The organic species examined include glucose, HMMA, and PEG-400. The analyte
 283 concentrations for each solution are listed in Table S1. For glucose, NE ranges from
 284 0.70 to 1.1 %, while the corresponding sulfate ranges from 0.23 to 0.70 %, with NE
 285 varying with solution composition. Results for additional organic species are provided
 286 in Figure S3 and Text S1. The NE determined using this offline method is higher than
 287 that reported by O'Brien et al. (2019) and comparable to values reported by Niedek et
 288 al. (2023) (Table 1). We note that Fang et al. (2015) reported substantially higher
 289 efficiencies (47–60 %) using the same nebulizer for XRF analysis of water-soluble
 290 elements. This difference arises primarily because the AMS samples only a small
 291 fraction of the nebulized air (6.2 % in this study), while Fang et al. (2015) quantified
 292 the full nebulized output.



293 Table 1. Summary of offline AMS methods for OA characterization and comparison with this study.

Filter Type	Extraction Solvent	Nebulizer	Required Volume	Particle Mode Diameter ^b	Nebulization Efficiency	Internal Standard	Detection Limit ^g	Bulk recovery ^g	Reference
quartz	Water, methanol, and ethyl acetate	Custom-built	N/A	~ 300 nm ^e	N/A	Phthalic acid	N/A	N/A	Mihara and Mochida (2011)
quartz	Water	Custom-built	5–15 mL	~ 200 nm ^d	3.8 mL/m ^{3f}	Sulfate	0.8 µg	64–76 %	Daellenbach et al. (2016)
N/A ^a	N/A ^a	Ultrasonic	N/A	~ 100 nm ^d	N/A	Sulfate	N/A	77–88 %	Xu et al. (2017)
quartz and PTFE	Water and methanol	Custom-built	2–4 µL	~ 150–200 nm ^e	0.02–0.06 %	Isotopically labeled nitrate	N/A	N/A	O'Brien et al. (2019)
PTFE	Methanol-water mixture	Custom-built	10 µL	~ 100–200 nm ^d	0.93–1.2 %	Isotopically labeled sulfate	2.2 ng ^h	N/A	Niedek et al. (2023)
quartz	Water	TSI	N/A	~ 100–200 nm ^e	N/A	N/A	N/A	N/A	Vasilakopoulou et al. (2023)
quartz	Water, methanol, and acetone	Apex Q	N/A	N/A	N/A	Isotopically labeled nitrate and sulfate	3–16 µg ⁱ	12–85 % ^j	Khare et al. (2025)
PTFE	Methanol-water mixture	Ultrasonic	2 mL	120–180 nm ^e	0.70–1.1 %	Sulfate	1.7 µg	53 ± 25 %	This study

294 Notes:

295 ^a Xu et al. (2017) use a Particle-into-Liquid Sampler (PILS) to convert ambient PM directly into aqueous extracts, rather than collecting particles on filters followed by
 296 solvent extraction as in most offline studies; N/A indicates not reported or not applicable.

297 ^b Particle size comparisons across studies should be interpreted with caution due to differences in solvent composition, concentration, and measurement techniques,
 298 including AMS, Scanning Mobility Particle Sizer (SMPS), hygroscopicity tandem differential mobility analyzer (HTDMA), and Zetasizer.

299 ^c Electrical mobility diameter.

300 ^d Vacuum aerodynamic diameter.



- 301 ^e Hydrodynamic diameter.
- 302 ^f The Unit is reported as $\text{mL}_{\text{solution}}/\text{m}^3_{\text{air}}$ in the original study, representing the volume of extract solution (mL) consumed per cubic meter of carrier air entering the AMS.
- 303 ^g Results are reported for OA unless explicitly stated; detection limits are expressed as mass per filter based on blank measurements unless otherwise noted.
- 304 ^h Detection limits are expressed as mass in solution, estimated using a standard binary solution containing sucrose and sulfate, each at a concentration of 0.06 mg/L.
- 305 ⁱ Results reported for OC.

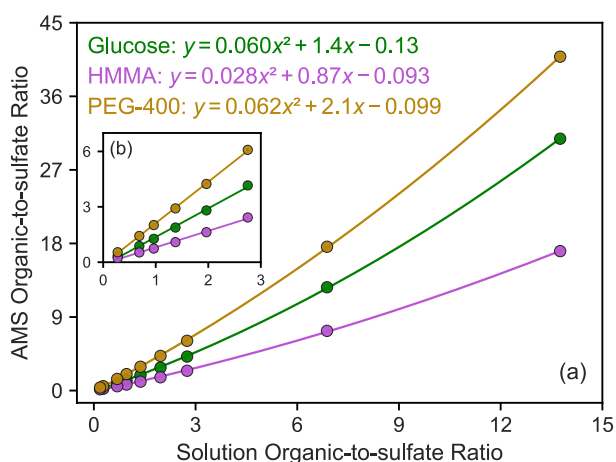


306 Variability in NE and the nonlinearity between nebulized and measured mass
307 necessitate the use of an internal standard (IS) to quantify organic concentrations. In
308 offline AMS studies, the IS should be non-refractory, soluble, chemically unreactive,
309 distinguishable from other sample components, internally mixed with organics, and
310 experience consistent and quantifiable nebulization processes (O'Brien et al., 2019).
311 The organic-to-IS ratio determined from AMS signals can then be used to correct for
312 any variations in NE and AMS sensitivity. The IS can be either an inorganic ion
313 originally present in the extract that can be independently quantified, or a species
314 externally spiked into the solution prior to nebulization at a known concentration. IS
315 used in previous studies includes sulfate (Daellenbach et al., 2016; Li et al., 2021),
316 nitrate (Srivastava et al., 2021), externally added isotopically labeled ammonium
317 sulfate or ammonium nitrate (Casotto et al., 2022; Cui et al., 2024; Khare et al., 2025),
318 and externally added phthalic acid (Mihara and Mochida, 2011). In this study, we select
319 sulfate as the internal standard because it is consistently present in samples, water-
320 soluble, nonvolatile, non-refractory, and independently quantified by both AMS and IC
321 within SPARTAN. Limitations of this approach are discussed below.

322 Figure 2 shows calibration curves for glucose, HMMA, and PEG-400 using sulfate as
323 the internal standard. To cover organic-to-sulfate ratios characteristic of urban
324 background PM, we vary the ratios in solution from 0.18 to 14. We observe strong
325 linearity ($r^2 > 0.996$) for organic-to-sulfate ratios between 0.28 and 2.8 in solution,
326 while nonlinearity appears at higher ratios. This likely reflects increased AMS
327 collection efficiency as organic-coated particles are more likely to adhere upon impact
328 with the vaporizer (Matthew et al., 2008; Xu et al., 2018). Compared with previous
329 offline AMS studies, this work explicitly considers nonlinearity in the calibration
330 relationship. Given the diverse properties of PM across globally distributed SPARTAN
331 sites, extending the organic-to-IS ratio range and accounting for nonlinearity are
332 therefore important for robust OA quantification.



333 Within the linear range (Figure 2b), we find slopes of 1.6, 0.89, and 2.2 for glucose,
334 HMMA, and PEG-400, respectively. These slopes reflect the ratio of the AMS RIE of
335 each organic compound to the RIE of sulfate. For complex organic mixtures, the most
336 accurate calibration would ideally use standards comprised of the average chemical
337 composition of ambient OA. However, such representation is challenging given the
338 chemical diversity and spatiotemporal variability of atmospheric OA. For urban
339 background aerosol, an RIE of 1.4 is commonly applied for OA (Canagaratna et al.,
340 2007; Xu et al., 2018), and an RIE of 0.97 for sulfate was determined from the
341 experiment-specific calibration in this study, corresponding to an organic-to-sulfate
342 RIE ratio of approximately 1.4. Given that the glucose-derived slope (1.6) is consistent
343 with this ratio, we select glucose-based calibration to approximate bulk OA in our
344 samples. Accordingly, we apply the nonlinear calibration function derived from glucose
345 in subsequent OA calculations for this offline method, with the associated uncertainty
346 propagated as described in Text S2.



347

348 Figure 2. The organic-to-sulfate ratio in known solutions compared to that
349 determined by AMS for three binary solutions (glucose, DL-4-Hydroxy-3-
350 methoxymandelic acid (HMMA), and poly(ethylene glycol) (PEG-400)) across
351 nine sulfate-organic combinations at a total solute concentration of 40 mg/L. The



352 main panel (a) shows quadratic fits to all data, with fitted equations annotated for
353 each compound. The inset (b) shows the corresponding linear relationships for six
354 ratios within the solution range of 0.28–2.8. Data are displayed as mean and
355 standard error from 8–12 replicate runs. Standard errors plotted as vertical error
356 bars are on the order of 10^{-2} and imperceptible at the scale of the figure.

357 Using sulfate as an internal standard, the quantification procedure for the offline AMS
358 method is summarized as follows. Each filter extract (2 mL) generates 8–12 AMS runs
359 (1 minute time resolution) using the optimized nebulization system. For each run k , the
360 blank-corrected AMS concentration for species i is calculated as:

$$361 \Delta I_{i,k} = I_{i,k} - \bar{I}_{i,LB} \quad (1)$$

362 where $I_{i,k}$ is the measured AMS concentration ($\mu\text{g}/\text{m}^3$) and $\bar{I}_{i,LB}$ is the measured mean
363 laboratory blank concentration for the corresponding cartridge ($\mu\text{g}/\text{m}^3$).

364 For each filter extract, the organic-to-sulfate ratio measured by AMS is calculated as
365 the mean of the ratios across N runs:

$$366 \phi_k = \frac{\Delta I_{OA,k}}{\Delta I_{sulfate,k}} \quad (2)$$

$$367 \phi_{AMS} = \frac{1}{N} \sum_{k=1}^N \phi_k \quad (3)$$

368 where ϕ_k is the organic-to-sulfate ratio for each run k and ϕ_{AMS} is the organic-to-sulfate
369 ratio for each filter extract in AMS.

370 Assuming an internal mixture with consistent behavior of sulfate and OA during
371 nebulization, ϕ_{AMS} is converted to the organic-to-sulfate ratio in the extract, $\phi_{extract}$, using
372 the inverse nonlinear calibration function $f(\phi_{AMS})$ in Figure 2. The offline OA
373 concentration ($C_{OA,offline}$, $\mu\text{g}/\text{m}^3$) is then calculated as:

$$374 \phi_{extract} = f(\phi_{AMS}) \quad (4)$$

$$375 C_{OA,offline} = \phi_{extract} \cdot C_{sulfate,extract} \cdot V_{extract} \cdot \frac{1}{V_{air}} \quad (5)$$

376 where $C_{sulfate,extract}$ is the sulfate concentration in extract determined by IC ($\mu\text{g}/\text{mL}$),
377 $V_{extract}$ is the extract volume (mL), and V_{air} is the sampled air volume (m^3). Uncertainties



378 in these parameters are propagated to estimate the overall uncertainty in the offline OA
379 concentration (Text S2).

380 The detection limit is defined as three times the standard deviation of blank
381 measurements. For offline AMS, which includes ultrapure water blanks, field blanks,
382 and laboratory blanks (Section 2.3), we calculate detection limits for each blank type
383 and adopt the largest value as a conservative estimate (Table S2). The resulting
384 detection limits are 1.7 μg for OA and 0.43 μg for sulfate, expressed as mass on filters.
385 Approximately 99.8 % of filters collected in SPARTAN exceed the sulfate detection
386 limit, indicating the suitability of this offline method to SPARTAN and its potential for
387 application in other monitoring networks.

388 **3.3 Evaluation with online AMS and other measurements**

389 **3.3.1 Online-offline sample collection**

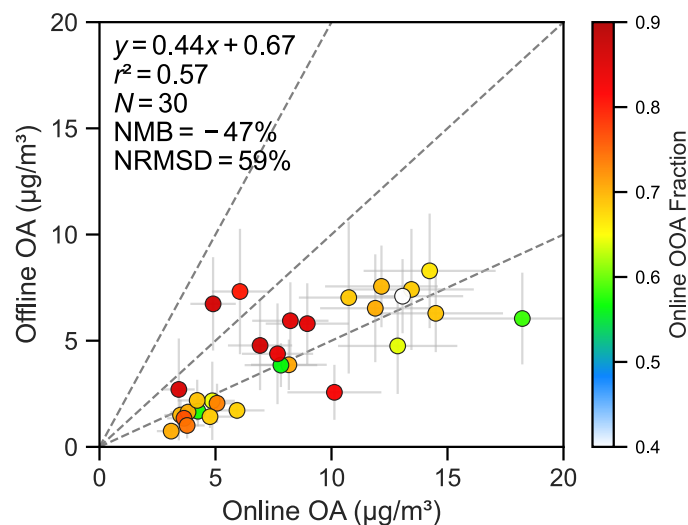
390 To evaluate the offline methodology, we conducted a pilot study by comparing OA
391 concentrations determined by the offline method with co-located online AMS
392 measurements. PM samples were collected from September to November 2025 on the
393 Danforth Campus (38.65° N, 90.31° W) of Washington University in St. Louis,
394 Missouri, US. Sampling was conducted by drawing air through a stainless-steel
395 sampling line from a third-floor rooftop located away from primary aerosol sources to
396 represent an urban background environment. Use of a single sampling line ensures
397 consistent air sampling for both the offline and online configurations in a controlled
398 laboratory environment. Filter sampling was performed using standard SPARTAN
399 stations operating continuously, with 24-hour sampling at flow rates ranging from 6 to
400 11 L/min. These flows enable the collected filters to primarily capture particles within
401 the effective size range of $\text{PM}_{2.5}$ and PM_{1} , given the PM_{1} size cut of the cyclone at 11
402 L/min and the $\text{PM}_{2.5}$ size cut at 5 L/min. In total, six cartridges were sampled, yielding
403 a collection of 42 paired filter samples, along with six paired field blanks. Collected
404 filters were analyzed using the HR-ToF-AMS following the offline methodology



405 described in [Section 2.3](#), and 30 paired filter samples exceeded offline detection limits
406 and are retained for further analysis. Concurrently, the same AMS with a standard PM₁
407 aerodynamic lens was operated alongside filter sampling from the same sampling line
408 to provide continuous online measurements of non-refractory PM₁. Blanks were
409 obtained by periodically inserting a high-efficiency particulate air (HEPA) filter
410 upstream of the cyclone during the campaign. Average online OA concentrations over
411 the duration of each filter sampling period were compared with the corresponding
412 offline filter measurements. Together, this setup enables a direct comparison between
413 offline filter-based measurements and co-located online AMS measurements. Previous
414 online-offline comparisons often have mismatches in instrument configurations (offline
415 AMS and online aerosol chemical speciation monitor (ACSM)), particle size cuts (PM₁₀
416 (aerodynamic diameter <10 μm), PM_{2.5}, and PM₁), and sampling time or location,
417 which can introduce additional uncertainty. In contrast, this study uses the same
418 sampling line and the same AMS instrument for both measurements, minimizing
419 potential interferences and providing a robust basis for comparison.

420 **3.3.2 Online-offline comparison**

421 [Figure 3](#) compares bulk OA concentrations derived from the offline AMS method with
422 those measured by the co-located online AMS. Most samples show lower
423 concentrations in offline AMS, with two exceptions that may reflect measurement
424 uncertainty. The OA recovery is 53 ± 25 % (mean \pm standard deviation), with a median
425 recovery of 48 % (38 % and 61 % for the first and third quartiles, respectively). For
426 complex mixtures such as ambient OA, recovery depends on the water solubility of its
427 numerous compounds ([Daellenbach et al., 2016](#)). Previous offline studies using water
428 extraction have reported a wide range of bulk OA recoveries, from 29 % in the polluted
429 city of Handan and 47 % in Beijing during wintertime in Northern China ([Li et al., 2021](#);
430 [Qiu et al., 2019](#)) to 64–76 % for PM collected in Paris and Zurich ([Daellenbach et al.,](#)
431 [2016](#)). Thus, it reflects both the efficiency of the offline method and intrinsic OA
432 properties that vary with composition and sources.



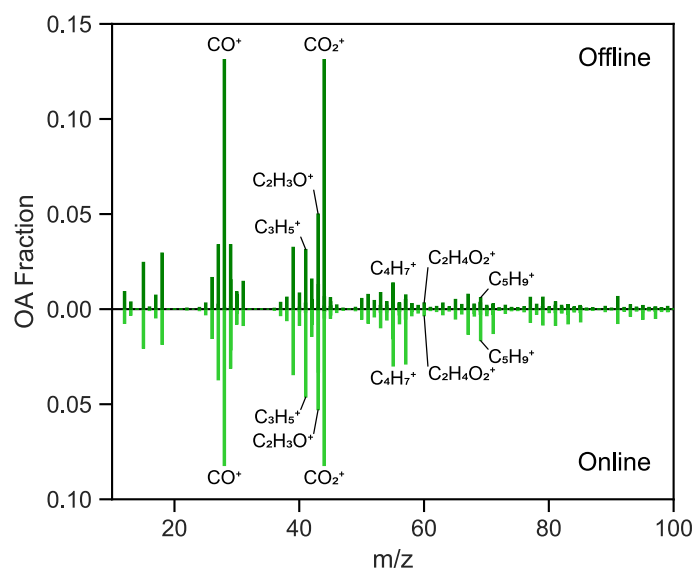
433

434 Figure 3. Comparison of online OA mass concentrations directly measured by the
 435 AMS with offline OA concentrations derived from filter samples analyzed using
 436 the offline method for samples collected in St. Louis. Online OA represents the
 437 time-averaged concentration over each corresponding filter sampling interval, with
 438 horizontal bars indicating the estimated AMS measurement uncertainty following
 439 Bahreini et al. (2009). Offline OA concentrations are calculated using sulfate as the
 440 internal standard and the nonlinear glucose calibration function, with vertical bars
 441 indicating the propagated uncertainty of offline OA concentrations. Each point
 442 presents the mean across 8 to 12 runs. Points are colored by the oxygenated OA
 443 (OOA) fraction determined from positive matrix factorization (PMF) of the online
 444 measurements. Annotations indicate the ordinary least-squares fit (y), coefficient
 445 of determination (r^2), number of comparison points (N), Normalized Mean Bias
 446 (NMB), and Normalized Root Mean Square Deviation (NRMSD). Dashed lines
 447 indicate reference lines with slopes of 0.5, 1, and 2.

448 To evaluate how well the offline AMS analysis preserves ambient OA composition, we
 449 compare average mass spectra from online and offline measurements (Figure 4). The



450 spectra show strong agreement, with an r^2 of 0.85. Similarly, Niedek et al. (2023) found
451 an r^2 of 0.70 for mass spectra collected in north-central Oklahoma, US, and
452 Daellenbach et al. (2016) found an $r^2 > 0.97$ for mass spectra from Zurich, both
453 comparing offline AMS with online ACSM measurements. Despite the overall
454 agreement, differences are observed in the relative contributions of individual ions,
455 suggesting that certain species may be preferentially recovered during filter collection,
456 extraction, and nebulization. To better understand compositional differences, OA
457 recovery is further examined by grouping ions into representative chemical families
458 following Daellenbach et al. (2016). Fragments are classified into mono-oxygenated
459 ions ($\text{CHO}_{z=1}$), poly-oxygenated ions ($\text{CHO}_{z>1}$), saturated hydrocarbons (CH_{sat}), and
460 unsaturated hydrocarbons (CH_{unsat}). Recovery varies substantially across ion families
461 (Figure S4). The highest recovery (mean \pm standard deviation) is observed for $\text{CHO}_{z>1}$
462 family (80 ± 35 %), dominated by organic acids, followed by $\text{CHO}_{z=1}$ family ($48 \pm$
463 21 %), likely representing alcohols, aldehydes, and ketones. In contrast, hydrocarbon-
464 like families have lower recoveries, with 37 ± 20 % for CH_{unsat} and 25 ± 16 % for CH_{sat} .
465 N-containing hydrocarbon ions (CHN) contribute only a small fraction of total OA and
466 are therefore not explicitly examined.



467

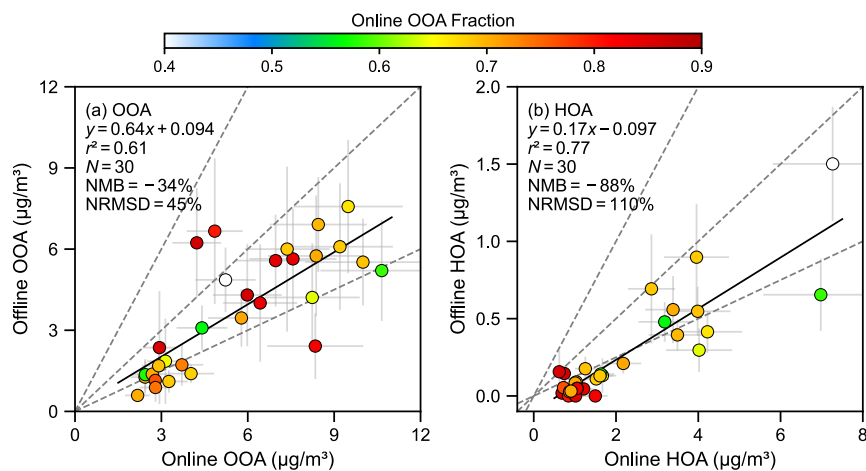
468 Figure 4. Comparison of average OA mass spectral fractions from online
469 measurements (bottom panel, light green) obtained directly by the AMS and offline
470 measurements (top panel, dark green) analyzed using the offline method for
471 samples collected in St. Louis. Fragments (m/z) commonly considered as source-
472 specific markers are explicitly labeled with their formula.

473 In addition to individual ions, we evaluate the recovery of OA factors. First, we perform
474 PMF analysis on online measurements and resolve two OA factors: oxygenated OA
475 (OOA) and hydrocarbon-like OA (HOA) (Figure S5). This two-factor solution is
476 selected for its physical interpretability and stable splitting and mixing behavior,
477 providing a broadly applicable framework for future applications (Figure S6). The
478 resulting factor profiles are consistent with established spectral characteristics, with
479 OOA dominated by oxygenated fragments at m/z 44 (CO₂⁺) and 43 (mostly C₂H₃O⁺)
480 and HOA characterized by alkyl fragments (C_nH_{2n+1}⁺ and C_nH_{2n-1}⁺) (Cubison et al.,
481 2011; Ng et al., 2010). These online-derived factor profiles are then used as a priori
482 constraints in the offline analysis. Offline factor concentrations are quantified by
483 applying weighted non-negative least squares (NNLS) regression to the offline mass



484 spectra using these factor profiles. The coefficients are constrained to be non-negative,
485 and measurement uncertainties are incorporated as weights to minimize the residual
486 between observed and reconstructed signals (Wang and Hopke, 1989). We perform
487 weighted NNLS on offline OA mass spectra for each run, and the mean factor
488 concentration across runs within a filter is used to represent the offline factor
489 contributions for that filter (see details in Text S3).

490 Figure 5 compares online and offline concentrations for OOA and HOA. OOA exhibits
491 relatively high recovery (mean \pm standard deviation) of 64 ± 28 % and a median of 59 %
492 (49 % and 79 % for the first and third quartiles, respectively). In contrast, HOA recovery
493 is substantially lower, with a mean and standard deviation of 9.9 ± 7.1 % and a median
494 of 8.5 % (4.6 % and 14 % for the first and third quartiles, respectively). These results
495 are consistent with the range reported in the literature (Figure 6), with OOA exhibiting
496 relatively high and consistent recovery, while other factors show lower and more
497 variable recovery. For example, Daellenbach et al. (2016) found recoveries of 89 % for
498 OOA and 11 % for HOA for PM collected in Paris and Zurich. Xu et al. (2017) reported
499 that 77 %, 96 %, and 68 % of isoprene-OA, more oxidized OOA (MO-OOA), and less
500 oxidized OOA (LO-OOA), respectively, are water-soluble in Atlanta, while HOA is
501 largely water-insoluble. Li et al. (2021) found recoveries of 49 % for OOA, 37 % for
502 biomass burning OA (BBOA), and 17 % for coal combustion OA (COA) in Handan,
503 northern China. Together, these observations align with the established understanding
504 of chemical characteristics of different OA components, with water solubility
505 decreasing from highly oxygenated species to more hydrocarbon-like species (Kondo
506 et al., 2007; Saxena and Hildemann, 1996).



507

508

509

510

511

512

513

514

515

516

517

518

519

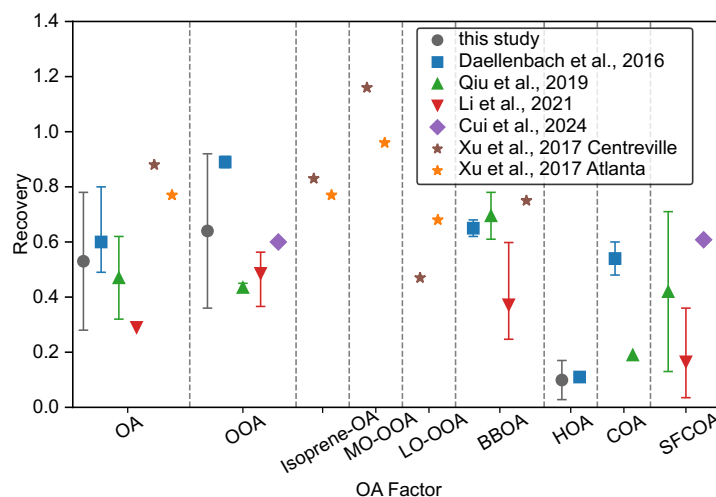
520

521

522

523

Figure 5. Comparison of online and offline factor contributions for (a) oxygenated OA (OOA) and (b) hydrocarbon-like OA (HOA) for samples collected in St. Louis. Online concentrations are calculated from positive matrix factorization (PMF) factor contributions and time-averaged bulk concentrations over each corresponding filter sampling interval, with horizontal bars indicating the estimated AMS measurement uncertainty. Offline concentrations are calculated using factor contributions derived from weighted non-negative least-squares (NNLS) regression with fixed factor profiles from online PMF, and multiplied by offline bulk OA concentrations determined using the offline method, with vertical bars indicating the propagated uncertainty of offline OA concentrations. Each point presents the mean across 8 to 12 runs. Points are colored by the OOA fraction determined from online PMF. Annotations indicate the ordinary least-squares fit (y), coefficient of determination (r^2), number of comparison points (N), Normalized Mean Bias (NMB), and Normalized Root Mean Square Deviation (NRMSD). Dashed lines indicate reference lines with slopes of (a) 0.5, 1, and 2 and (b) 0.125, 0.25, and 0.5.



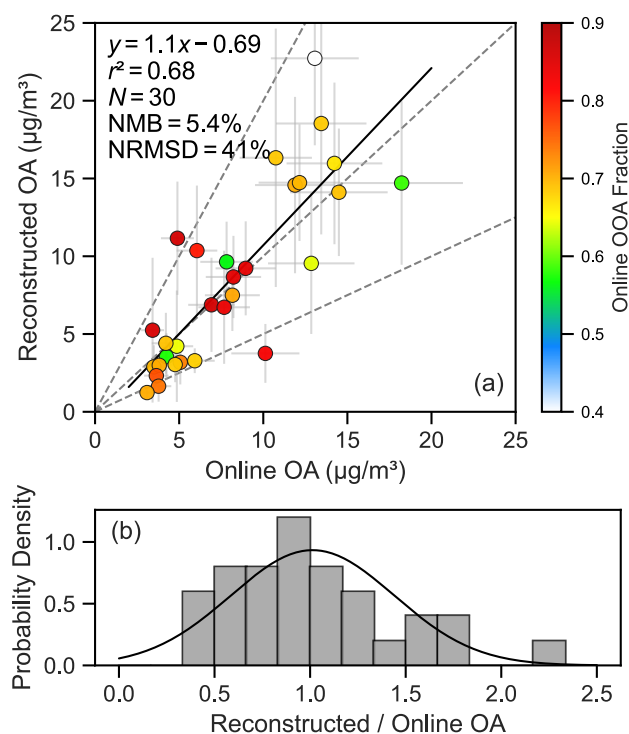
524

525 Figure 6. Comparison of OA recovery reported in the literature and in this study
 526 across bulk OA and major OA factors, including oxygenated OA (OOA), isoprene-
 527 derived OA (isoprene-OA), more-oxidized OOA (MO-OOA), less-oxidized OOA
 528 (LO-OOA), biomass burning OA (BBOA), hydrocarbon-like OA (HOA), cooking
 529 OA (COA), and solid fuel combustion OA (SFCOA). Symbols indicate different
 530 studies. Original values from each study are shown, so direct comparison should
 531 be interpreted with caution due to differences in statistical measures across studies.
 532 This study is reported as mean \pm standard deviation, Daellenbach et al. (2016) as
 533 median with first and third quartiles, Qiu et al. (2019) as mean \pm standard deviation,
 534 Li et al. (2021) as median with the 10th and 90th percentiles, Cui et al. (2024) as
 535 mean values, and Xu et al. (2017) as mode. For studies reporting ranges only, the
 536 central value is taken as the midpoint of the reported range.

537 Building on the factor-resolved recovery, we reconstruct OA by weighting each offline-
 538 derived factor by its mean recovery and compare it with online OA measurements
 539 (Figure 7). This approach aligns with the objectives of this offline method and
 540 monitoring networks such as SPARTAN for long-term ambient OA characterization.
 541 This comparison shows an r^2 of 0.68 and a Normalized Mean Bias (NMB) of 5.4 %.
 542 When evaluated over longer timescales such as at the cartridge level of one week,



543 agreement improves further, with r^2 increasing to 0.84 and NMB decreasing to 2.2 %
 544 (Figure S7). These results highlight that offline measurements can provide reliable
 545 estimates of ambient OA concentrations, particularly over longer periods.



546

547 Figure 7. (a) Comparison of reconstructed OA concentrations with online OA
 548 concentrations for samples collected in St. Louis. Reconstructed OA
 549 concentrations are calculated by dividing each offline-derived factor by its mean
 550 mean recovery. Online OA represents the time-averaged concentration over each
 551 corresponding filter sampling interval. Horizontal bars indicate the estimated AMS
 552 measurement uncertainty of online OA concentrations, while vertical bars indicate
 553 the propagated uncertainty of offline OA concentrations. Each point presents the
 554 mean across 8 to 12 runs. Points are colored by the oxygenated OA (OOA) fraction
 555 determined from positive matrix factorization (PMF) of the online measurements.



556 Annotations indicate the ordinary least-squares fit (y), coefficient of determination
557 (r^2), number of comparison points (N), Normalized Mean Bias (NMB), and
558 Normalized Root Mean Square Deviation (NRMSD). Dashed lines indicate
559 reference lines with slopes of 0.5, 1, and 2. (b) Histogram of the ratio of
560 reconstructed to online OA for the same samples. The fitted curve represents a
561 smoothed probability density function of this ratio.

562 As an additional evaluation, sulfate, ammonium, and nitrate concentrations derived
563 from the offline AMS are compared with co-located online AMS and complementary
564 offline IC and XRF measurements. Sulfate shows strong agreement across
565 measurement techniques, including online AMS, IC measurements of water extracts,
566 and XRF measurements of filter samples, with r^2 of 0.80 and 0.95 for the respective
567 comparisons (Figure S8a and S8b). Since offline AMS sulfate is intrinsically linked to
568 IC sulfate through its use as the internal standard, the two are treated equivalently in
569 this comparison. The observed agreement suggests a minor contribution from
570 organosulfur compounds in the collected samples and supports the use of sulfate as the
571 internal standard, as further discussed in Section 3.4. Offline AMS-derived ammonium
572 and nitrate are quantified using sulfate as the internal standard, following the same
573 approach as for OA but assuming a unity calibration slope between ammonium-to-
574 sulfate and nitrate-to-sulfate ratios in the extract and in the AMS. We find strong
575 agreement in ammonium concentrations between offline AMS and IC, with a slope of
576 1.1 and r^2 of 0.93 (Figure S8d), supporting the reliability of the offline quantification.
577 Additional comparisons with other measurements are provided in Text S4.

578 **3.4 Uncertainty in the application to SPARTAN**

579 To support the goal of characterizing ambient OA across SPARTAN using
580 reconstructed OA, we evaluate additional sources of uncertainty beyond those
581 quantified for offline OA in the St. Louis online-offline comparison samples.
582 Specifically, we assess the applicability of sulfate as an internal standard across
583 SPARTAN sites and the variability in OOA and HOA factor profiles and recoveries.



584 We use sulfate as the internal standard to leverage its routine measurements in most
585 monitoring networks. Two potential concerns should be noted. First, sulfate
586 concentrations have declined in many regions over time, which may influence its
587 suitability as a reference species (Tsimpidi et al., 2025). Second, part of the AMS
588 sulfate signal may arise from organosulfur compounds rather than inorganic sulfate
589 measured by IC. However, these factors appear to have limited influence in this study.
590 The first concern is mitigated by both IC and AMS providing low detection limits for
591 sulfate, by retaining only samples with sulfate concentrations above the detection limits,
592 and by increasing sulfate in many regions targeted by SPARTAN. The second concern
593 is addressed by comparing water-soluble inorganic sulfate measured by IC with total
594 particulate sulfur measured by XRF to identify and exclude future samples that may
595 contain large contributions from organosulfur compounds. Therefore, errors associated
596 with using sulfate as the internal standard are expected to be small.

597 We focus on the two most broadly applicable OA factors, OOA and HOA, to provide
598 a simple but robust framework suitable for application across diverse SPARTAN sites.
599 For the St. Louis online-offline comparison samples, offline factor contributions are
600 quantified using weighted NNLS regression with fixed factor profiles derived from co-
601 located online AMS measurements. However, such site-specific, highly accurate factor
602 profiles may not be available at many SPARTAN locations with limited AMS
603 observations. To evaluate this limitation, we use the AMS Spectral Database to identify
604 four additional pairs of deconvoluted OOA and HOA factor profiles (Ulbrich et al.,
605 2009a, 2009b, 2009c), derived from studies conducted in the US (Zhang et al., 2005),
606 Zurich (Lanz et al., 2008), China (Elser et al., 2016), and an average across five sites
607 (Ng et al., 2011). These profiles represent variability in factor spectra and are applied
608 as fixed priors in weighted NNLS regression for the St. Louis offline samples. The
609 resulting four sets of offline OOA and HOA, together with the original set based on co-
610 located measurements, are then extrapolated using recoveries to reconstruct ambient
611 OA. Factor recovery varies with time and location, indicating that recovery estimates



612 derived at one site may not be directly applicable to other sites (Li et al., 2021;
613 Vasilakopoulou et al., 2023). We consider this variability in two ways. First, previous
614 studies suggest that OOA recovery is relatively consistent across sites (Figure 6).
615 Second, we define conservative recovery ranges by synthesizing results from this and
616 previous offline AMS studies, yielding 0.36–0.92 for OOA and 0.028–0.17 for HOA.
617 A sensitivity analysis is performed by bootstrapping OOA and HOA recoveries 100
618 times from these ranges for five sets of factor profiles across 30 samples for
619 reconstruction. Despite variability in factor profiles and the use of broad recovery
620 ranges, the distribution of reconstructed-to-online OA ratios exhibits a mode between
621 0.8 and 1.2 (Figure S9), supporting the feasibility of future extrapolation of offline OA
622 measurements to characterize ambient OA across SPARTAN sites.

623 4. Conclusions

624 This study presents a comprehensive development and evaluation of an offline AMS
625 methodology and demonstrates its applicability to filter-based measurement networks.
626 The commercial nebulization system enables continuous aerosol generation from small
627 sample volumes of 2 mL and is straightforward and reproducible to operate,
628 representing a substantial improvement for large-scale sample processing. Use of
629 sulfate as an internal standard leverages routine sulfate measurements in monitoring
630 networks. Offline AMS results are directly evaluated against co-located online
631 measurements using the same sampling line and instrument. The online-offline
632 comparison shows varying recovery across OA factors, with the highest recovery
633 observed for OOA, likely due to its higher water solubility. Therefore, this offline
634 method provides a robust estimate of oxygenated species, although correction is
635 required when estimating hydrocarbon-like species associated with more primary
636 emissions. Despite source-dependent recovery biases, the offline method reliably
637 represents ambient OA concentrations, supporting its application in monitoring
638 networks and enabling the development of a consistent OA dataset across globally

<https://doi.org/10.5194/egusphere-2026-2663>

Preprint. Discussion started: 21 May 2026

© Author(s) 2026. CC BY 4.0 License.



639 distributed sites. Future work will apply this method to the Surface Particulate Matter

640 Network to examine globally distributed variation in OA.



641 **Data availability**

642 All datasets are available upon request from Lu Xu (xu1@wustl.edu) and Randall V. Martin
643 (rvmartin@wustl.edu)

644 **Author contributions**

645 YR designed the study, conducted the experiments, analyzed the data, and drafted the
646 manuscript. RVM secured funding, co-designed the study, edited the manuscript, and provided
647 guidance throughout the analysis. JHC contributed to AMS instrument maintenance and
648 nebulizer optimization. CRO assisted with SPARTAN operations. BJW contributed to AMS
649 instrument maintenance. RJW assisted with the ultrasonic nebulizer. LX contributed to AMS
650 measurements, co-designed the study, edited the manuscript, and provided guidance
651 throughout the analysis. All authors reviewed and approved the final manuscript.

652 **Acknowledgements**

653 This work was supported by the Clean Air Fund Grant 001591 and the National Science
654 Foundation Grant 2020673. The authors thank William A. Brooks (Aerodyne Research, Inc.)
655 for technical support and assistance with the AMS.

656 **References**

657 Bahreini, R., Ervens, B., Middlebrook, A.M., Warneke, C., de Gouw, J.A., DeCarlo, P.F.,
658 Jimenez, J.L., Brock, C.A., Neuman, J.A., Ryerson, T.B., Stark, H., Atlas, E., Brioude, J., Fried,
659 A., Holloway, J.S., Peischl, J., Richter, D., Walega, J., Weibring, P., Wollny, A.G., and
660 Fehsenfeld, F.C.: Organic aerosol formation in urban and industrial plumes near Houston and
661 Dallas, Texas, *J. Geophys. Res.-Atmos.*, 114, D00F16, 2009.

662 Bates, J.T., Fang, T., Verma, V., Zeng, L.H., Weber, R.J., Tolbert, P.E., Abrams, J.Y., Sarnat,
663 S.E., Klein, M., Mulholland, J.A., and Russell, A.G.: Review of acellular assays of ambient
664 particulate matter oxidative potential: Methods and relationships with composition, sources,
665 and health effects, *Environ. Sci. Technol.*, 53, 4003–4019, 2019.



- 666 Bhowmik, H.S., Tripathi, S.N., Shukla, A.K., Lalchandani, V., Murari, V., Devaprasad, M.,
667 Shivam, A., Bhushan, R., Prevot, A.S.H., and Rastogi, N.: Contribution of fossil and biomass-
668 derived secondary organic carbon to winter water-soluble organic aerosols in Delhi, India, *Sci.*
669 *Total Environ.*, 912, 168655, 2024.
- 670 Bozzetti, C., Daellenbach, K.R., Hueglin, C., Fermo, P., Sciare, J., Kasper-Giebl, A., Mazar,
671 Y., Abbaszade, G., El Kazzi, M., Gonzalez, R., Shuster-Meiseles, T., Flasch, M., Wolf, R.,
672 Krepelova, A., Canonaco, F., Schnelle-Kreis, J., Slowik, J.G., Zimmermann, R., Rudich, Y.,
673 Baltensperger, U., El Haddad, I., and Prevot, A.S.H.: Size-resolved identification,
674 characterization, and quantification of primary biological organic aerosol at a European rural
675 site, *Environ. Sci. Technol.*, 50, 3425–3434, 2016.
- 676 Bozzetti, C., Sosedova, Y., Xiao, M., Daellenbach, K.R., Ulevicius, V., Dudoitis, V., Mordas,
677 G., Bycenkiene, S., Plauskaite, K., Vlachou, A., Golly, B., Chazeau, B., Besombes, J.-L.,
678 Baltensperger, U., Jaffrezo, J.-L., Slowik, J.G., El Haddad, I., and Prevot, A.S.H.: Argon
679 offline-AMS source apportionment of organic aerosol over yearly cycles for an urban, rural,
680 and marine site in northern Europe, *Atmos. Chem. Phys.*, 17, 117–141, 2017a.
- 681 Bozzetti, C., El Haddad, I., Salameh, D., Daellenbach, K.R., Fermo, P., Gonzalez, R.,
682 Minguillon, M.C., Iinuma, Y., Poulain, L., Elser, M., Muller, E., Slowik, J.G., Jaffrezo, J.-L.,
683 Baltensperger, U., Marchand, N., and Prevot, A.S.H.: Organic aerosol source apportionment
684 by offline-AMS over a full year in Marseille, *Atmos. Chem. Phys.*, 17, 8247–8268, 2017b.
- 685 Canagaratna, M.R., Jayne, J.T., Jimenez, J.L., Allan, J.D., Alfarra, M.R., Zhang, Q., Onasch,
686 T.B., Drewnick, F., Coe, H., Middlebrook, A., Delia, A., Williams, L.R., Trimborn, A.M.,
687 Northway, M.J., DeCarlo, P.F., Kolb, C.E., Davidovits, P., and Worsnop, D.R.: Chemical and
688 microphysical characterization of ambient aerosols with the aerodyne aerosol mass
689 spectrometer, *Mass Spectrom. Rev.*, 26, 185–222, 2007.
- 690 Cash, J.M., Di Marco, C., Langford, B., Heal, M.R., Mandal, T.K., Sharma, S.K., Gurjar, B.R.,
691 and Nemitz, E.: Response of organic aerosol to Delhi’s pollution control measures over the
692 period 2011–2018, *Atmos. Environ.*, 315, 120123, 2023.



- 693 Casotto, R., Kusan, A.C., Bhattu, D., Cui, T., Manousakas, M.I., Frka, S., Kroflic, A., Grgic,
694 I., Ciglenecki, I., Baltensperger, U., Slowik, J.G., Daellenbach, K.R., and Prevot, A.S.H.:
695 Chemical composition and sources of organic aerosol on the Adriatic coast in Croatia, *Atmos.*
696 *Environ. X*, 13, 100159, 2022.
- 697 Casotto, R., Skiba, A., Rauber, M., Strahl, J., Tobler, A., Bhattu, D., Lamkaddam, H.,
698 Manousakas, M., Salazar, G., Cui, T.Q., Canonaco, F., Samek, L., Rys, A., El Haddad, I.,
699 Kasper-Giebl, A., Baltensperger, U., Necki, J., Szidat, S., Styszko, K., Slowik, J.G., Prevot,
700 A.S.H., and Daellenbach, K.R.: Organic aerosol sources in Krakow, Poland, before
701 implementation of a solid fuel residential heating ban, *Sci. Total Environ.*, 855, 158655, 2023.
- 702 Chen, Y., Xu, L., Humphry, T., Hettiyadura, A.P.S., Ovadnevaite, J., Huang, S., Poulain, L.,
703 Schroder, J.C., Campuzano-Jost, P., Jimenez, J.L., Herrmann, H., O'Dowd, C., Stone, E.A.,
704 and Ng, N.L.: Response of the aerodyne aerosol mass spectrometer to inorganic sulfates and
705 organosulfur compounds: Applications in field and laboratory measurements, *Environ. Sci.*
706 *Technol.*, 53, 5176–5186, 2019.
- 707 Chung, C.E., Ramanathan, V., and Decremmer, D.: Observationally constrained estimates of
708 carbonaceous aerosol radiative forcing, *Proc. Natl. Acad. Sci. USA*, 109, 11624–11629, 2012.
- 709 Cubison, M.J., Ortega, A.M., Hayes, P.L., Farmer, D.K., Day, D., Lechner, M.J., Brune, W.H.,
710 Apel, E., Diskin, G.S., Fisher, J.A., Fuelberg, H.E., Hecobian, A., Knapp, D.J., Mikoviny, T.,
711 Riemer, D., Sachse, G.W., Sessions, W., Weber, R.J., Weinheimer, A.J., Wisthaler, A., and
712 Jimenez, J.L.: Effects of aging on organic aerosol from open biomass burning smoke in aircraft
713 and laboratory studies, *Atmos. Chem. Phys.*, 11, 12049–12064, 2011.
- 714 Cui, T., Manousakas, M.I., Wang, Q., Uzu, G., Hao, Y., Khare, P., Qi, L., Chen, Y., Han, Y.,
715 Slowik, J.G., Jaffrezo, J.-L., Cao, J., Prevot, A.S.H., and Daellenbach, K.R.: Composition and
716 sources of organic aerosol in two megacities in western China using complementary mass
717 spectrometric and statistical techniques, *Environ. Sci. Technol. Air*, 1, 1053–1065, 2024.
- 718 Daellenbach, K.R., Bozzetti, C., Krepelova, A., Canonaco, F., Wolf, R., Zotter, P., Fermo, P.,
719 Crippa, M., Slowik, J.G., Sosedova, Y., Zhang, Y., Huang, R.J., Poulain, L., Szidat, S.,



- 720 Baltensperger, U., El Haddad, I., and Prevot, A.S.H.: Characterization and source
721 apportionment of organic aerosol using offline aerosol mass spectrometry, *Atmos. Meas. Tech.*,
722 9, 23–39, 2016.
- 723 Daellenbach, K.R., Stefenelli, G., Bozzetti, C., Vlachou, A., Fermo, P., Gonzalez, R.,
724 Piazzalunga, A., Colombi, C., Canonaco, F., Hueglin, C., Kasper-Giebl, A., Jaffrezo, J.-L.,
725 Bianchi, F., Slowik, J.G., Baltensperger, U., El Haddad, I., and Prevot, A.S.H.: Long-term
726 chemical analysis and organic aerosol source apportionment at nine sites in central Europe:
727 Source identification and uncertainty assessment, *Atmos. Chem. Phys.*, 17, 13265–13282,
728 2017.
- 729 Debus, B., Weakley, A.T., Takahama, S., George, K.M., Amiri-Farahani, A., Schichtel, B.,
730 Copeland, S., Wexler, A.S., and Dillner, A.M.: Quantification of major particulate matter
731 species from a single filter type using infrared spectroscopy – application to a large-scale
732 monitoring network, *Atmos. Meas. Tech.*, 15, 2685–2702, 2022.
- 733 DeCarlo, P.F., Kimmel, J.R., Trimborn, A., Northway, M.J., Jayne, J.T., Aiken, A.C., Gonin,
734 M., Fuhrer, K., Horvath, T., Docherty, K.S., Worsnop, D.R., and Jimenez, J.L.: Field-
735 deployable, high-resolution, time-of-flight aerosol mass spectrometer, *Anal. Chem.*, 78, 8281–
736 8289, 2006.
- 737 Dillner, A.M. and Takahama, S.: Predicting ambient aerosol thermal-optical reflectance
738 measurements from infrared spectra: Elemental carbon, *Atmos. Meas. Tech.*, 8, 4013–4023,
739 2015.
- 740 Elser, M., Huang, R.J., Wolf, R., Slowik, J.G., Wang, Q., Canonaco, F., Li, G., Bozzetti, C.,
741 Daellenbach, K.R., Huang, Y., Zhang, R., Li, Z., Cao, J., Baltensperger, U., El Haddad, I., and
742 Prevot, A.S.H.: New insights into PM_{2.5} chemical composition and sources in two major cities
743 in China during extreme haze events using aerosol mass spectrometry, *Atmos. Chem. Phys.*,
744 16, 3207–3225, 2016.
- 745 Fang, T., Guo, H., Verma, V., Peltier, R. E., and Weber, R. J.: PM_{2.5} water-soluble elements in
746 the southeastern United States: Automated analytical method development, spatiotemporal



747 distributions, source apportionment, and implications for health studies, *Atmos. Chem. Phys.*,
748 15, 11667–11682, 2015.

749 Ge, X., Li, L., Chen, Y., Chen, H., Wu, D., Wang, J., Xie, X., Ge, S., Ye, Z., Xu, J., and Chen,
750 M.: Aerosol characteristics and sources in Yangzhou, China resolved by offline aerosol mass
751 spectrometry and other techniques, *Environ. Pollut.*, 225, 74–85, 2017.

752 Huang, R.J., Zhang, Y., Bozzetti, C., Ho, K.F., Cao, J.J., Han, Y., Daellenbach, K.R., Slowik,
753 J.G., Platt, S.M., Canonaco, F., Zotter, P., Wolf, R., Pieber, S.M., Bruns, E.A., Crippa, M.,
754 Ciarelli, G., Piazzalunga, A., Schwikowski, M., Abbaszade, G., Schnelle-Kreis, J.,
755 Zimmermann, R., An, Z., Szidat, S., Baltensperger, U., El Haddad, I., and Prevot, A.S.H.: High
756 secondary aerosol contribution to particulate pollution during haze events in China, *Nature*,
757 514, 218–222, 2014.

758 Jeon, S., Walker, M.J., Sueper, D.T., Day, D.A., Handschy, A.V., Jimenez, J.L., and Williams,
759 B.J.: A searchable database and mass spectral comparison tool for the Aerosol Mass
760 Spectrometer (AMS) and the Aerosol Chemical Speciation Monitor (ACSM), *Atmos. Meas.*
761 *Tech.*, 16, 6075–6095, 2023.

762 Jimenez, J.L., Jayne, J.T., Shi, Q., Kolb, C.E., Worsnop, D.R., Yourshaw, I., Seinfeld, J.H.,
763 Flagan, R.C., Zhang, X.F., Smith, K.A., Morris, J.W., and Davidovits, P.: Ambient aerosol
764 sampling using the aerodyne aerosol mass spectrometer, *J. Geophys. Res.-Atmos.*, 108, 8425,
765 2003.

766 Jimenez, J.L., Canagaratna, M.R., Donahue, N.M., Prevot, A.S.H., Zhang, Q., Kroll, J.H.,
767 DeCarlo, P.F., Allan, J.D., Coe, H., Ng, N.L., Aiken, A.C., Docherty, K.S., Ulbrich, I.M.,
768 Grieshop, A.P., Robinson, A.L., Duplissy, J., Smith, J.D., Wilson, K.R., Lanz, V.A., Hueglin,
769 C., Sun, Y.L., Tian, J., Laaksonen, A., Raatikainen, T., Rautiainen, J., Vaattovaara, P., Ehn,
770 M., Kulmala, M., Tomlinson, J.M., Collins, D.R., Cubison, M.J., Dunlea, E.J., Huffman, J.A.,
771 Onasch, T.B., Alfarra, M.R., Williams, P.I., Bower, K., Kondo, Y., Schneider, J., Drewnick,
772 F., Borrmann, S., Weimer, S., Demerjian, K., Salcedo, D., Cottrell, L., Griffin, R., Takami, A.,
773 Miyoshi, T., Hatakeyama, S., Shimono, A., Sun, J.Y., Zhang, Y.M., Dzepina, K., Kimmel, J.R.,



- 774 Sueper, D., Jayne, J.T., Herndon, S.C., Trimborn, A.M., Williams, L.R., Wood, E.C.,
775 Middlebrook, A.M., Kolb, C.E., Baltensperger, U., and Worsnop, D.R.: Evolution of organic
776 aerosols in the atmosphere, *Science*, 326, 1525–1529, 2009.
- 777 Kanakidou, M., Seinfeld, J.H., Pandis, S.N., Barnes, I., Dentener, F.J., Facchini, M.C., Van
778 Dingenen, R., Ervens, B., Nenes, A., Nielsen, C.J., Swietlicki, E., Putaud, J.P., Balkanski, Y.,
779 Fuzzi, S., Horth, J., Moortgat, G.K., Winterhalter, R., Myhre, C.E.L., Tsigaridis, K., Vignati,
780 E., Stephanou, E.G., and Wilson, J.: Organic aerosol and global climate modelling: A review,
781 *Atmos. Chem. Phys.*, 5, 1053–1123, 2005.
- 782 Khare, P., Kurdieh, A.A., Hao, Y.F., Manousakas, M.I., Dada, L., Tobler, A., Schneider-
783 Beltran, K., Diapouli, E., Skiba, A., Styszko, K., Slowik, J.G., Prevot, A.S.H., and Daellenbach,
784 K.R.: Organic solvents-based offline aerosol mass spectrometry (SOFF-AMS) for
785 comprehensive chemical characterization of ambient organic aerosol, *Environ. Sci. Technol.*,
786 59, 18236–18248, 2025.
- 787 Kondo, Y., Miyazaki, Y., Takegawa, N., Miyakawa, T., Weber, R.J., Jimenez, J.L., Zhang, Q.,
788 and Worsnop, D.R.: Oxygenated and water-soluble organic aerosols in Tokyo, *J. Geophys.*
789 *Res.-Atmos.*, 112, D01203, 2007.
- 790 Kroll, J.H. and Seinfeld, J.H.: Chemistry of secondary organic aerosol: Formation and
791 evolution of low-volatility organics in the atmosphere, *Atmos. Environ.*, 42, 3593–3624, 2008.
- 792 Kroll, J.H., Donahue, N.M., Jimenez, J.L., Kessler, S.H., Canagaratna, M.R., Wilson, K.R.,
793 Altieri, K.E., Mazzoleni, L.R., Wozniak, A.S., Bluhm, H., Mysak, E.R., Smith, J.D., Kolb, C.E.,
794 and Worsnop, D.R.: Carbon oxidation state as a metric for describing the chemistry of
795 atmospheric organic aerosol, *Nat. Chem.*, 3, 133–139, 2011.
- 796 Lanz, V.A., Alfarra, M.R., Baltensperger, U., Buchmann, B., Hueglin, C., Szidat, S., Wehrli,
797 M.N., Wacker, L., Weimer, S., Caseiro, A., Puxbaum, H., and Prevot, A.S.H.: Source
798 attribution of submicron organic aerosols during wintertime inversions by advanced factor
799 analysis of aerosol mass spectra, *Environ. Sci. Technol.*, 42, 214–220, 2008.



- 800 Li, H., Zhang, Q., Jiang, W., Collier, S., Sun, Y., Zhang, Q., and He, K.: Characteristics and
801 sources of water-soluble organic aerosol in a heavily polluted environment in Northern China,
802 *Sci. Total Environ.*, 758, 143970, 2021.
- 803 Liu, P.S.K., Deng, R., Smith, K.A., Williams, L.R., Jayne, J.T., Canagaratna, M.R., Moore, K.,
804 Onasch, T.B., Worsnop, D.R., and Deshler, T.: Transmission efficiency of an aerodynamic
805 focusing lens system: Comparison of model calculations and laboratory measurements for the
806 aerodyne aerosol mass spectrometer, *Aerosol Sci. Technol.*, 41, 721–733, 2007.
- 807 Liu, X., Turner, J.R., Oxford, C.R., McNeill, J., Walsh, B., Le Roy, E., Weagle, C.L., Stone,
808 E., Zhu, H., Liu, W., Wei, Z., Hyslop, N.P., Giacomo, J., Dillner, A.M., Salam, A., Hossen,
809 A.-A., Islam, Z., Abboud, I., Akoshile, C., Amador-Munoz, O., Anh, N.X., Asfaw, A.,
810 Balasubramanian, R., Chang, R.Y.W., Coburn, C., Dey, S., Diner, D.J., Dong, J., Farrah, T.,
811 Gahungu, P., Garland, R.M., Grutter de la Mora, M., Hasheminassab, S., John, J., Kim, J., Kim,
812 J.S., Langerman, K., Lee, P.C., Lestari, P., Liu, Y., Mamo, T., Martins, M., Mayol-Bracero,
813 O.L., Naidoo, M., Park, S.S., Schechner, Y., Schofield, R., Tripathi, S.N., Windwer, E., Wu,
814 M.T., Zhang, Q., Brauer, M., Rudich, Y., and Martin, R.V.: Elemental characterization of
815 ambient particulate matter for a globally distributed monitoring network: Methodology and
816 implications, *Environ. Sci. Technol. Air*, 1, 283–293, 2024.
- 817 Matthew, B.M., Middlebrook, A.M., and Onasch, T.B.: Collection efficiencies in an aerodyne
818 aerosol mass spectrometer as a function of particle phase for laboratory generated aerosols,
819 *Aerosol Sci. Technol.*, 42, 884–898, 2008.
- 820 McNeill, J., Snider, G., Weagle, C.L., Walsh, B., Bissonnette, P., Stone, E., Abboud, I.,
821 Akoshile, C., Anh, N.X., Balasubramanian, R., Brook, J.R., Coburn, C., Cohen, A., Dong, J.L.,
822 Gagnon, G., Garland, R.M., He, K.B., Holben, B.N., Kahn, R., Kim, J.S., Lagrosas, N., Lestari,
823 P., Liu, Y., Jeba, F., Joy, K.S., Martins, J.V., Misra, A., Norford, L.K., Quel, E.J., Salam, A.,
824 Schichtel, B., Tripathi, S.N., Wang, C., Zhang, Q., Brauer, M., Gibson, M.D., Rudich, Y., and
825 Martin, R.V.: Large global variations in measured airborne metal concentrations driven by
826 anthropogenic sources, *Sci. Rep.*, 10, 21817, 2020.



- 827 Middlebrook, A.M., Bahreini, R., Jimenez, J.L., and Canagaratna, M.R.: Evaluation of
828 composition-dependent collection efficiencies for the aerodyne aerosol mass spectrometer
829 using field data, *Aerosol Sci. Technol.*, 46, 258–271, 2012.
- 830 Mihara, T. and Mochida, M.: Characterization of solvent-extractable organics in urban aerosols
831 based on mass spectrum analysis and hygroscopic growth measurement, *Environ. Sci. Technol.*,
832 45, 9168–9174, 2011.
- 833 Moschos, V., Dzepina, K., Bhattu, D., Lamkaddam, H., Casotto, R., Daellenbach, K.R.,
834 Canonaco, F., Rai, P., Aas, W., Becagli, S., Calzolari, G., Eleftheriadis, K., Moffett, C.E.,
835 Schnelle-Kreis, J., Severi, M., Sharma, S., Skov, H., Vestenius, M., Zhang, W., Hakola, H.,
836 Hellen, H., Huang, L., Jaffrezo, J.-L., Massling, A., Nojgaard, J.K., Petaja, T., Popovicheva,
837 O., Sheesley, R.J., Traversi, R., Yttri, K.E., Schmale, J., Prevot, A.S.H., Baltensperger, U., and
838 El Haddad, I.: Equal abundance of summertime natural and wintertime anthropogenic Arctic
839 organic aerosols, *Nat. Geosci.*, 15, 196–202, 2022.
- 840 Ng, N.L., Canagaratna, M.R., Zhang, Q., Jimenez, J.L., Tian, J., Ulbrich, I.M., Kroll, J.H.,
841 Docherty, K.S., Chhabra, P.S., Bahreini, R., Murphy, S.M., Seinfeld, J.H., Hildebrandt, L.,
842 Donahue, N.M., DeCarlo, P.F., Lanz, V.A., Prevot, A.S.H., Dinar, E., Rudich, Y., and Worsnop,
843 D.R.: Organic aerosol components observed in Northern Hemispheric datasets from aerosol
844 mass spectrometry, *Atmos. Chem. Phys.*, 10, 4625–4641, 2010.
- 845 Ng, N.L., Canagaratna, M.R., Jimenez, J.L., Zhang, Q., Ulbrich, I.M., and Worsnop, D.R.:
846 Real-time methods for estimating organic component mass concentrations from Aerosol Mass
847 Spectrometer data, *Environ. Sci. Technol.*, 45, 910–916, 2011.
- 848 Niedeck, C.R., Mei, F., Zawadowicz, M.A., Zhu, Z., Schmid, B., and Zhang, Q.: Quantitative
849 chemical assay of nanogram-level particulate matter using aerosol mass spectrometry:
850 Characterization of particles collected from uncrewed atmospheric measurement platforms,
851 *Atmos. Meas. Tech.*, 16, 955–968, 2023.
- 852 Niedeck, C.R., Mei, F., Jiang, W., Trousdell, J., Zawadowicz, M.A., Schmid, B., and Zhang, Q.:
853 Advancing aerosol chemical characterization and vertical profiling over the Southern Great



- 854 Plains using uncrewed aerial sampling and offline Aerosol Mass Spectrometry, *Environ. Sci.*
855 *Technol. Air*, 2, 2131–2146, 2025.
- 856 O’Brien, R.E., Ridley, K.J., Canagaratna, M.R., Jayne, J.T., Croteau, P.L., Worsnop, D.R.,
857 Budisulistiorini, S.H., Surratt, J.D., Follett, C.L., Repeta, D.J., and Kroll, J.H.: Ultrasonic
858 nebulization for the elemental analysis of microgram-level samples with offline aerosol mass
859 spectrometry, *Atmos. Meas. Tech.*, 12, 1659–1671, 2019.
- 860 Ohata, S., Moteki, N., and Kondo, Y.: Evaluation of a method for measurement of the
861 concentration and size distribution of black carbon particles suspended in rainwater, *Aerosol*
862 *Sci. Technol.*, 45, 1326–1336, 2011.
- 863 Paatero, P. and Tapper, U.: Positive matrix factorization – a nonnegative factor model with
864 optimal utilization of error-estimates of data values, *Environmetrics*, 5, 111–126, 1994.
- 865 Paatero, P. and Hopke, P.K.: Rotational tools for factor analytic models, *J. Chemometr.*, 23,
866 91–100, 2009.
- 867 Pai, S.J., Heald, C.L., Pierce, J.R., Farina, S.C., Marais, E.A., Jimenez, J.L., Campuzano-Jost,
868 P., Nault, B.A., Middlebrook, A.M., Coe, H., Shilling, J.E., Bahreini, R., Dingle, J.H., and Vu,
869 K.: An evaluation of global organic aerosol schemes using airborne observations, *Atmos. Chem.*
870 *Phys.*, 20, 2637–2665, 2020.
- 871 Qiu, Y., Xie, Q., Wang, J., Xu, W., Li, L., Wang, Q., Zhao, J., Chen, Y., Chen, Y., Wu, Y., Du,
872 W., Zhou, W., Lee, J., Zhao, C., Ge, X., Fu, P., Wang, Z., Worsnop, D.R., and Sun, Y.: Vertical
873 characterization and source apportionment of water-soluble organic aerosol with high-
874 resolution aerosol mass spectrometry in Beijing, China, *ACS Earth and Space Chem.*, 3, 273–
875 284, 2019.
- 876 Ren, Y., Oxford, C.R., Zhang, D., Liu, X., Zhu, H., Dillner, A.M., White, W.H., Chakrabarty,
877 R.K., Hasheminassab, S., Diner, D.J., Le Roy, E.J., Kumar, J., Viteri, V., Song, K., Akoshile,
878 C., Amador-Munoz, O., Asfaw, A., Chang, R.Y.W., Francis, D., Gahungu, P., Garland, R.M.,
879 Grutter, M., Kim, J., Langerman, K., Lee, P.C., Lestari, P., Mayol-Bracero, O.L., Naidoo, M.,
880 Nelli, N., O’Neill, N., Park, S.S., Salam, A., Sarangi, B., Schechner, Y., Schofield, R., Tripathi,



- 881 S.N., Windwer, E., Wu, M.T., Zhang, Q., Rudich, Y., Brauer, M., and Martin, R.V.: Black
882 carbon emissions generally underestimated in the global south as revealed by globally
883 distributed measurements, *Nat. Commun.*, 16, 7010, 2025.
- 884 Sareen, N., Schwier, A.N., Lathem, T.L., Nenes, A., and McNeill, V.F.: Surfactants from the
885 gas phase may promote cloud droplet formation, *Proc. Natl. Acad. Sci. USA*, 110, 2723–2728,
886 2013.
- 887 Saxena, P. and Hildemann, L.M.: Water-soluble organics in atmospheric particles: A critical
888 review of the literature and application of thermodynamics to identify candidate compounds,
889 *J. Atmos. Chem.*, 24, 57–109, 1996.
- 890 Shrivastava, M., Cappa, C.D., Fan, J., Goldstein, A.H., Guenther, A.B., Jimenez, J.L., Kuang,
891 C., Laskin, A., Martin, S.T., Ng, N.L., Petaja, T., Pierce, J.R., Rasch, P.J., Roldin, P., Seinfeld,
892 J.H., Shilling, J., Smith, J.N., Thornton, J.A., Volkamer, R., Wang, J., Worsnop, D.R., Zaveri,
893 R.A., Zelenyuk, A., and Zhang, Q.: Recent advances in understanding secondary organic
894 aerosol: Implications for global climate forcing, *Rev. Geophys.*, 55, 509–559, 2017.
- 895 Snider, G., Weagle, C.L., Martin, R.V., van Donkelaar, A., Conrad, K., Cunningham, D.,
896 Gordon, C., Zwicker, M., Akoshile, C., Artaxo, P., Anh, N.X., Brook, J., Dong, J., Garland,
897 R.M., Greenwald, R., Griffith, D., He, K., Holben, B.N., Kahn, R., Koren, I., Lagrosas, N.,
898 Lestari, P., Ma, Z., Vanderlei Martins, J., Quel, E.J., Rudich, Y., Salam, A., Tripathi, S.N., Yu,
899 C., Zhang, Q., Zhang, Y., Brauer, M., Cohen, A., Gibson, M.D., and Liu, Y.: SPARTAN: A
900 global network to evaluate and enhance satellite-based estimates of ground-level particulate
901 matter for global health applications, *Atmos. Meas. Tech.*, 8, 505–521, 2015.
- 902 Snider, G., Weagle, C.L., Murdymootoo, K.K., Ring, A., Ritchie, Y., Stone, E., Walsh, A.,
903 Akoshile, C., Anh, N.X., Balasubramanian, R., Brook, J., Qonitan, F.D., Dong, J.L., Griffith,
904 D., He, K.B., Holben, B.N., Kahn, R., Lagrosas, N., Lestari, P., Ma, Z.W., Misra, A., Norford,
905 L.K., Quel, E.J., Salam, A., Schichtel, B., Segev, L., Tripathi, S., Wang, C., Yu, C., Zhang, Q.,
906 Zhang, Y.X., Brauer, M., Cohen, A., Gibson, M.D., Liu, Y., Martins, J.V., Rudich, Y., and



- 907 Martin, R.V.: Variation in global chemical composition of PM_{2.5}: Emerging results from
908 SPARTAN, *Atmos. Chem. Phys.*, 16, 9629–9653, 2016.
- 909 Srivastava, D., Daellenbach, K.R., Zhang, Y., Bonnaire, N., Chazeau, B., Perraudin, E., Gros,
910 V., Lucarelli, F., Villenave, E., Prevot, A.S.H., El Haddad, I., Favez, O., and Albinet, A.:
911 Comparison of five methodologies to apportion organic aerosol sources during a PM pollution
912 event, *Sci. Total Environ.*, 757, 143168, 2021.
- 913 Sun, Y., Zhang, Q., Zheng, M., Ding, X., Edgerton, E.S., and Wang, X.: Characterization and
914 source apportionment of water-soluble organic matter in atmospheric fine particles (PM_{2.5})
915 with High-Resolution Aerosol Mass Spectrometry and GC-MS, *Environ. Sci. Technol.*, 45,
916 4854–4861, 2011.
- 917 Sun, Y., Luo, H., Li, Y., Zhou, W., Xu, W., Fu, P., and Zhao, D.: Atmospheric organic aerosols:
918 Online molecular characterization and environmental impacts, *npj Clim. Atmos. Sci.*, 8, 305,
919 2025.
- 920 Tsimpidi, A.P., Scholz, S.M.C., Milouisis, A., Mihalopoulos, N., and Karydis, V.A.: Aerosol
921 composition trends during 2000–2020: In-depth insights from model predictions and multiple
922 worldwide near-surface observation datasets, *Atmos. Chem. Phys.*, 25, 10183–10213, 2025.
- 923 Tuet, W.Y., Fok, S., Verma, V., Rodriguez, M.S.T., Grosberg, A., Champion, J.A., and Ng,
924 N.L.: Dose-dependent intracellular reactive oxygen and nitrogen species (ROS/RNS)
925 production from particulate matter exposure: Comparison to oxidative potential and chemical
926 composition, *Atmos. Environ.*, 144, 335–344, 2016.
- 927 Ulbrich, I.M., Canagaratna, M.R., Zhang, Q., Worsnop, D.R., and Jimenez, J.L.: Interpretation
928 of organic components from Positive Matrix Factorization of aerosol mass spectrometric data,
929 *Atmos. Chem. Phys.*, 9, 2891–2918, 2009a.
- 930 Ulbrich, I.M., Handschy, A., Lechner, M., and Jimenez, J.L.: High-Resolution AMS Spectral
931 Database, <http://cires.colorado.edu/jimenez-group/HRAMSsd/>, (last access: 8 May 2026),
932 2009b.



- 933 Ulbrich, I.M., Handschy, A., Lechner, M., and Jimenez, J.L.: AMS Spectral Database,
934 <http://cires.colorado.edu/jimenez-group/AMSSd/>, (last access: 8 May 2026), 2009c.
- 935 Vasilakopoulou, C.N., Florou, K., Kaltsonoudis, C., Stavroulas, I., Mihalopoulos, N., and
936 Pandis, S.N.: Development and evaluation of an improved offline aerosol mass spectrometry
937 technique, *Atmos. Meas. Tech.*, 16, 2837–2850, 2023.
- 938 Vlachou, A., Daellenbach, K.R., Bozzetti, C., Chazeau, B., Salazar, G.A., Szidat, S., Jaffrezo,
939 J.-L., Hueglin, C., Baltensperger, U., El Haddad, I., and Prevot, A.S.H.: Advanced source
940 apportionment of carbonaceous aerosols by coupling offline AMS and radiocarbon size-
941 segregated measurements over a nearly 2-year period, *Atmos. Chem. Phys.*, 18, 6187–6206,
942 2018.
- 943 Vlachou, A., Tobler, A., Lamkaddam, H., Canonaco, F., Daellenbach, K.R., Jaffrezo, J.-L.,
944 Minguillon, M.C., Maasikmets, M., Teinmaa, E., Baltensperger, U., El Haddad, I., and Prevot,
945 A.S.H.: Development of a versatile source apportionment analysis based on positive matrix
946 factorization: A case study of the seasonal variation of organic aerosol sources in Estonia,
947 *Atmos. Chem. Phys.*, 19, 7279–7295, 2019.
- 948 Wang, D. and Hopke, P.K.: The use of constrained least-squares to solve the chemical mass
949 balance problem, *Atmos. Environ.*, 23, 2143–2150, 1989.
- 950 Weagle, C.L., Snider, G., Li, C., van Donkelaar, A., Philip, S., Bissonnette, P., Burke, J.,
951 Jackson, J., Latimer, R., Stone, E., Abboud, I., Akoshile, C., Anh, N.X., Brook, J.R., Cohen,
952 A., Dong, J., Gibson, M.D., Griffith, D., He, K., Holben, B.N., Kahn, R., Keller, C.A., Kim,
953 J.S., Lagrosas, N., Lestari, P., Khian, Y.L., Liu, Y., Marais, E.A., Martins, J.V., Misra, A.,
954 Muliane, U., Pratiwi, R., Quel, E.J., Salam, A., Segev, L., Tripathi, S.N., Wang, C., Zhang, Q.,
955 Brauer, M., Rudich, Y., and Martin, R.V.: Global sources of fine particulate matter:
956 Interpretation of PM_{2.5} chemical composition observed by SPARTAN using a global chemical
957 transport model, *Environ. Sci. Technol.*, 52, 11670–11681, 2018.



- 958 White, W.H., Trzepla, K., Hyslop, N.P., and Schichtel, B.A.: A critical review of filter
959 transmittance measurements for aerosol light absorption, and calibration for a decade of
960 monitoring on PTFE membranes, *Aerosol Sci. Technol.*, 50, 984–1002, 2016.
- 961 Williams, B.J., Goldstein, A.H., Millet, D.B., Holzinger, R., Kreisberg, N.M., Hering, S.V.,
962 White, A.B., Worsnop, D.R., Allan, J.D., and Jimenez, J.L.: Chemical speciation of organic
963 aerosol during the International Consortium for Atmospheric Research on Transport and
964 Transformation 2004: Results from in situ measurements, *J. Geophys. Res.-Atmos.*, 112,
965 D10S26, 2007.
- 966 Xu, J., Zhang, Q., Wang, Z., Yu, G., Ge, X., and Qin, X.: Chemical composition and size
967 distribution of summertime PM_{2.5} at a high altitude remote location in the northeast of the
968 Qinghai-Xizang (Tibet) Plateau: Insights into aerosol sources and processing in free
969 troposphere, *Atmos. Chem. Phys.*, 15, 5069–5081, 2015.
- 970 Xu, L., Guo, H., Weber, R.J., and Ng, N.L.: Chemical characterization of water-soluble organic
971 aerosol in contrasting rural and urban environments in the Southeastern United States, *Environ.*
972 *Sci. Technol.*, 51, 78–88, 2017.
- 973 Xu, W., Lambe, A., Silva, P., Hu, W., Onasch, T., Williams, L., Croteau, P., Zhang, X.,
974 Renbaum-Wolff, L., Fortner, E., Jimenez, J.L., Jayne, J., Worsnop, D., and Canagaratna, M.:
975 Laboratory evaluation of species-dependent relative ionization efficiencies in the aerodyne
976 aerosol mass spectrometer, *Aerosol Sci. Technol.*, 52, 626–641, 2018.
- 977 Ye, Z., Liu, J., Gu, A., Feng, F., Liu, Y., Bi, C., Xu, J., Li, L., Chen, H., Chen, Y., Dai, L.,
978 Zhou, Q., and Ge, X.: Chemical characterization of fine particulate matter in Changzhou, China,
979 and source apportionment with offline aerosol mass spectrometry, *Atmos. Chem. Phys.*, 17,
980 2573–2592, 2017a.
- 981 Ye, Z., Li, Q., Liu, J., Luo, S., Zhou, Q., Bi, C., Ma, S., Chen, Y., Chen, H., Li, L., and Ge, X.:
982 Investigation of submicron aerosol characteristics in Changzhou, China: Composition, source,
983 and comparison with co-collected PM, *Chemosphere*, 183, 176–185, 2017b.



984 Zhang, Q., Alfarra, M.R., Worsnop, D.R., Allan, J.D., Coe, H., Canagaratna, M.R., and
985 Jimenez, J.L.: Deconvolution and quantification of hydrocarbon-like and oxygenated organic
986 aerosols based on aerosol mass spectrometry, *Environ. Sci. Technol.*, 39, 4938–4952, 2005.

987 Zhang, Q., Jimenez, J.L., Canagaratna, M.R., Allan, J.D., Coe, H., Ulbrich, I., Alfarra, M.R.,
988 Takami, A., Middlebrook, A.M., Sun, Y.L., Dzepina, K., Dunlea, E., Docherty, K., DeCarlo,
989 P.F., Salcedo, D., Onasch, T., Jayne, J.T., Miyoshi, T., Shimo, A., Hatakeyama, S.,
990 Takegawa, N., Kondo, Y., Schneider, J., Drewnick, F., Borrmann, S., Weimer, S., Demerjian,
991 K., Williams, P., Bower, K., Bahreini, R., Cottrell, L., Griffin, R.J., Rautiainen, J., Sun, J.Y.,
992 Zhang, Y.M., and Worsnop, D.R.: Ubiquity and dominance of oxygenated species in organic
993 aerosols in anthropogenically-influenced Northern Hemisphere midlatitudes, *Geophys. Res.*
994 *Let.*, 34, L13801, 2007.